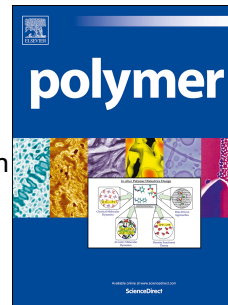


# Accepted Manuscript

Linear rheology of natural rubber compounds filled with silica, short nylon fiber or both

Yihu Song, Dengjia Huang



PII: S0032-3861(17)31141-2

DOI: [10.1016/j.polymer.2017.11.073](https://doi.org/10.1016/j.polymer.2017.11.073)

Reference: JPOL 20186

To appear in: *Polymer*

Received Date: 12 October 2017

Revised Date: 25 November 2017

Accepted Date: 27 November 2017

Please cite this article as: Song Y, Huang D, Linear rheology of natural rubber compounds filled with silica, short nylon fiber or both, *Polymer* (2017), doi: 10.1016/j.polymer.2017.11.073.

This is a PDF file of an unedited manuscript that has been accepted for publication. As a service to our customers we are providing this early version of the manuscript. The manuscript will undergo copyediting, typesetting, and review of the resulting proof before it is published in its final form. Please note that during the production process errors may be discovered which could affect the content, and all legal disclaimers that apply to the journal pertain.

## Graphical Abstract

1

2

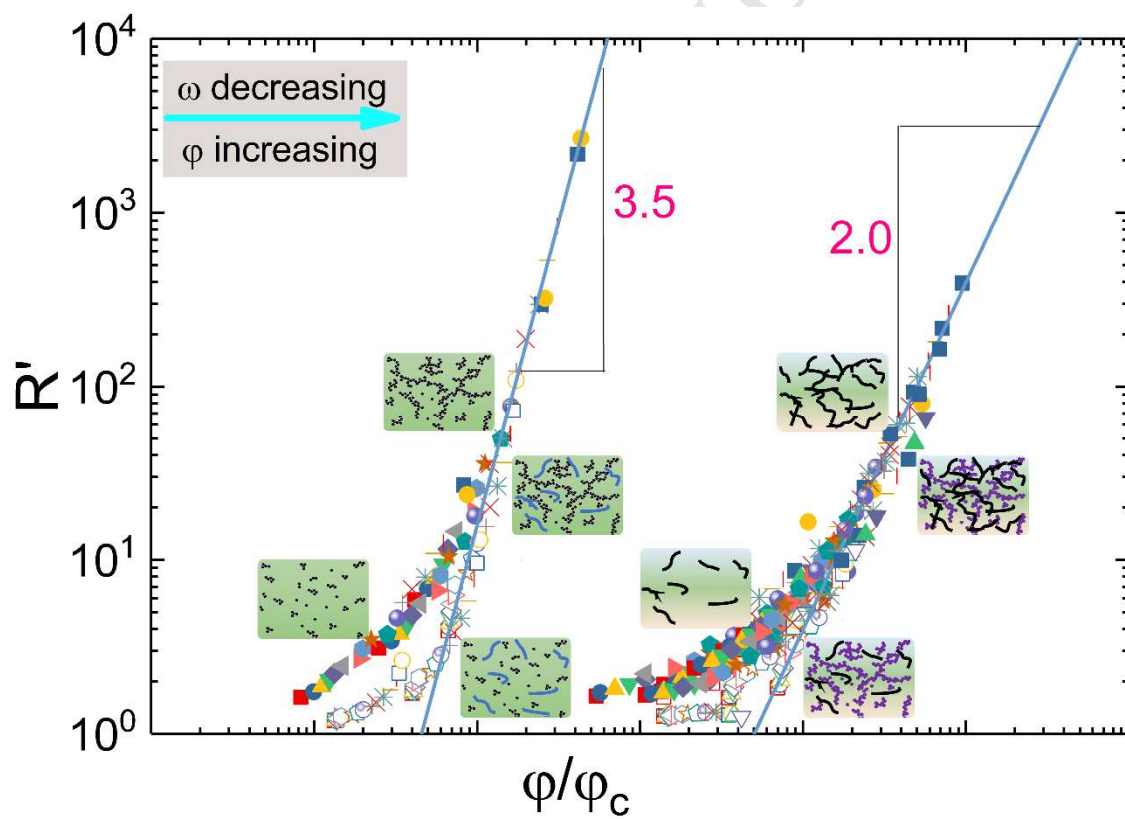
3 **Linear rheology of natural rubber compounds filled with silica, short**  
4 **nylon fiber or both**

5

6 Yihu Song, Dengjia Huang, Qiang Zheng

7

8 The time-concentration superpositioning principle is able to account for the reinforcement and  
9 dissipation of natural rubber filled with silica, short nylon fiber or both.



10

1 **Linear rheology of natural rubber compounds filled with silica,**  
2 **short nylon fiber or both**

3

4 Yihu Song\*, Dengjia Huang

5

6 MOE Key Laboratory of Macromolecular Synthesis and Functionalization, Department of  
7 Polymer Science and Engineering, Zhejiang University, Hangzhou 310027, China

8

9 **RUNNING TITLE: Linear rheology of NR compounds**

---

\* Corresponding author.

*E-mail address:* [s\\_yh0411@zju.edu.cn](mailto:s_yh0411@zju.edu.cn) (Y. Song).

1

2 **Abstract:** Engineered rubbery materials in practical applications usually contain nanoparticle  
3 and microscopic short fiber while no theories could describe the viscoelasticity of the  
4 compounds varying with these two kinds of fillers. We describe how the linear rheology of  
5 natural rubber compounds varies with the loading of precipitated silica, short nylon fiber, or  
6 both. We for the first time disclose a filler dimension-dependent hydrodynamic-to-non-  
7 hydrodynamic transition by applying the time-concentration superposition principle for  
8 accounting for the apparent liquid-to-solid transition related to filler composition and loading  
9 and the retarded dynamics of the matrix. A framework for simultaneous solving the  
10 reinforcement and dissipation of the multi-component compounds is suggested, providing a  
11 new perspective on understanding the filling effect for manufacturing high-performance  
12 rubber materials.

13 **Keywords:** Compounds; Rheology; Time-concentration superposition

14

15

1 Nanoparticles are extensively used to reinforce rubbers [1-4]. In engineered truck tread  
2 compounds, a low content of well dispersed short fibers is usually introduced to improve  
3 mechanical and dynamic properties. Both nanoparticles and short fibers could introduce a so-  
4 called liquid-to-solid transition that is importance for optimizing the compounding behaviors  
5 for developing high-performance materials for tires and other applications [5, 6]. While a  
6 range of efforts have been made to understand the filler reinforcement behavior in myriad  
7 publications in the open literature, few studies are focused on the synergistic effect of  
8 nanoparticles and microfibers on the linear rheology of the multi-component compounds [7]  
9 and there are lack of theories being able to predict the compounds' viscoelasticity as a  
10 function of filler composition and polymer dynamics. Herein we prepare natural rubber (NR)  
11 compounds filled with precipitated silica (PS), short nylon fiber (SNF) or both fillers. We  
12 investigate the rheological roles played by nanoparticles and microfibers for providing a better  
13 understanding of the reinforcement and dissipation mechanisms.

14 We prepared single- and two-filler compounds of NR (SVR3L, weight-averaged molecular  
15 weight  $1,120 \text{ kg mol}^{-1}$ , polydispersity index 3.57, polyisoprene content 98 %, Shanghai Duokang  
16 Ind. Co., Ltd., China) according to the formulations listed in Table 1. The single-filler  
17 compounds PS(NR) were prepared by mixing NR, PS (ZQ356; cetyltrimethyl ammonium  
18 bromide adsorption  $184 \text{ m}^2 \text{ g}^{-1}$ , dibutyl phthalate adsorption  $5.5 \text{ cm}^3 \text{ g}^{-1}$ , Zhuzhou Xinglong  
19 Chem. Ind. Co., Ltd., China), and silane bis( $\gamma$ -triethoxysilylpropyl)tetrasulfide (5 % in mass with  
20 respect to PS, Hangzhou Jessica Chem. Co., Ltd., China) in a torque rheometer (HAAKE, Thermo  
21 Scientific Co., USA) at  $150 \text{ }^\circ\text{C}$  and 60 rpm for 12 min. The two-filler compounds PS(SNF0.014)  
22 were prepared following the aforementioned procedure but a predetermined amount of  
23 SNF(NR)<sub>c</sub> was incorporated. The single-filler compounds SNF(NR)<sub>uc</sub> were prepared by mixing NR  
24 and short fibers of nylon 66 (N3/30,  $3.0 \pm 0.3 \text{ mm}$  in length, aspect ratio 160, Goonvean Fibres  
25 Ltd., UK) at  $50 \text{ }^\circ\text{C}$  for 12 min on a two-roll open mill (XK-160, Zhanjiang Rubber & Plastic

1 Machinery Co., Ltd., China). The single-filler compounds SNF(NR)<sub>c</sub> containing maleated natural  
 2 rubber by an amount of 10 parts per hundred NR were prepared following the same procedure.  
 3 The single-filler compounds SNF(NR)<sub>c</sub> with  $\varphi_{\text{SNF}}=0.07$  was diluted by NR to produce SNF(NR)<sub>d</sub>.  
 4 During the dilution procedure, the single-filler compound PS(NR) with  $\varphi_{\text{SNF}}=0.20$  was  
 5 introduced, yielding the two-filler compounds SNF(PS0.12)<sub>d</sub>. Antioxidant *N*-(1,3-dimethylbutyl)-  
 6 *N'*-phenyl-*p*-phenylenediamine (Changzhou Xince Polym. Mater. Co., Ltd., China) by an amount  
 7 of 1.6 parts per hundred NR was included in all the compounds.

8

9 **Table 1.** The filler compositions and main rheological parameters of the compounds.

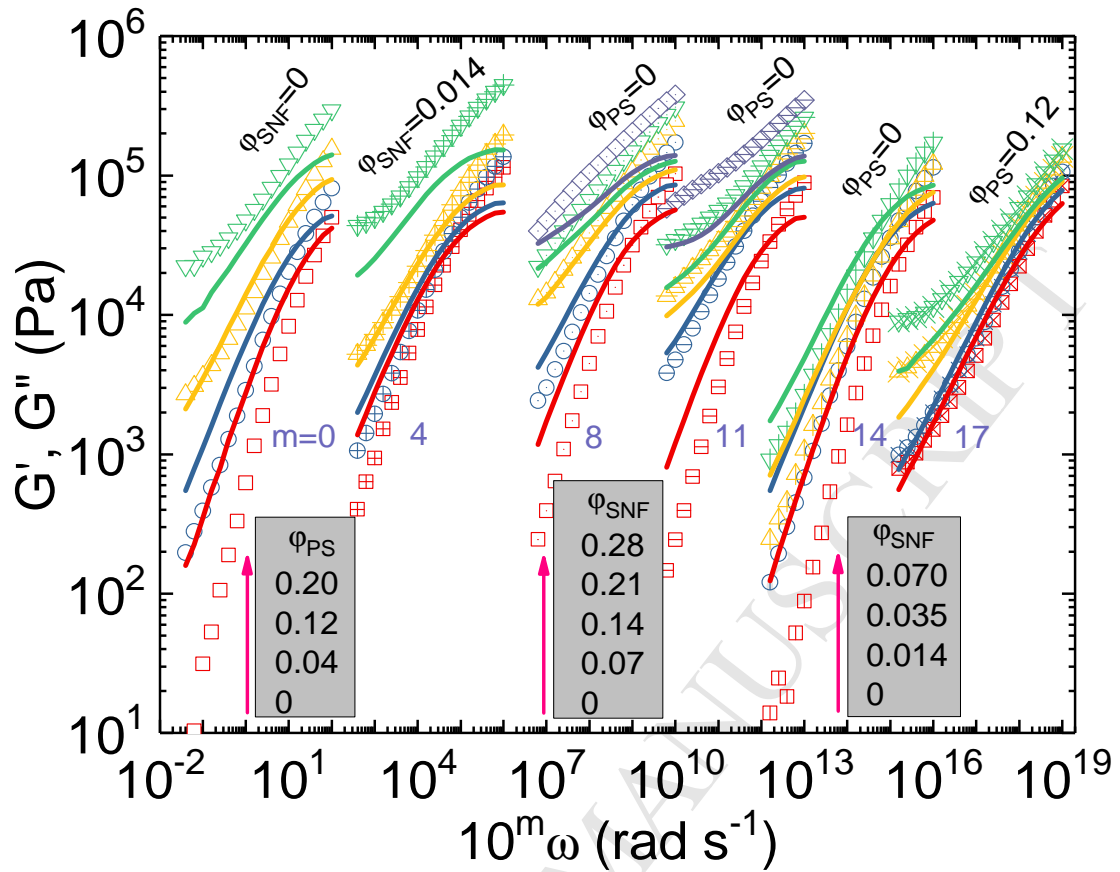
Compounds <sup>a</sup>	$\varphi_{\text{PS}}$	$\varphi_{\text{SNF}}$	$\tau_m$ (s) <sup>b</sup>	$\varphi_{\text{cm}}$ <sup>c</sup>
PS(NR)	0.04-0.20	0	0.01566	0.410
PS(SNF0.014)	0.04-0.20	0.014	0.15659	0.160
SNF(NR) <sub>uc</sub>	0	0.07-0.28	0.07937	0.340
SNF(NR) <sub>c</sub>	0	0.07-0.28	0.05682	0.290
SNF(NR) <sub>d</sub>	0	0.014-0.070	0.03472	0.165
SNF(PS0.12) <sub>d</sub>	0.12	0.014-0.070	0.14706	0.087

10 <sup>a</sup> The compounds are named as A(B) where A and B denote the filler and matrix. The latter may be  
 11 either pure rubber (NR) or filled rubber (SNF0.014 and PS0.12, containing 1.4% SNF and 12% PS in  
 12 volume fractions, respectively). The subscripts “uc” and “c” identify the uncompatibilized compounds  
 13 and those compatibilized with maleated natural rubber with 1.5% grafted maleic anhydride prepared *via*  
 14 a Nakason method [8]. The subscript “d” denotes the compounds prepared via the dilution method. <sup>b</sup>  
 15 Terminal relaxation time of the matrix determined at reciprocal of frequency at the  $G'_m(\omega)-G''_m(\omega)$   
 16 crossover for the single-filler compounds or by applying the modified two phase model for the two-filler  
 17 compounds. <sup>c</sup> Critical concentration for hydrodynamic-to-non-hydrodynamic regime transition at  
 18  $\omega=1/\tau_m$ .

19

1 The compounds after storage for more than one day were compressed into discs of 25 mm  
2 in diameter and 2 mm in thickness on a press vulcanizer (XL-25, Huzhou Xinli Rubber  
3 Machinery Co., Ltd., China) at  $100 \pm 5$  °C under 10 MPa for 10 min. A strain-controlled  
4 rheometer (ARES-G2, TA Instrument, USA) was used to measure dynamic rheological  
5 responses of the uncured compounds at 100 °C using a plate-plate geometry with a serrated  
6 surface texture to prevent slipping. Frequency ( $\omega$ ) sweeps from 100 to 0.0158 rad s<sup>-1</sup> were  
7 performed at 0.1 % dynamic strain amplitude located in the linearity regime (Fig. S1).

8 By introducing maleated natural rubber as compatibilizer and silane as coupling agent, both  
9 SNF and PS are well dispersed (Fig. S2). While both fillers do not influence glass transition  
10 temperature of the mobile rubber component (Fig. S3), they cause the liquid-to-solid transition  
11 (Fig. 1) as identified from appearance of plateaus of storage and loss moduli [ $G'(\omega, \varphi)$  and  
12  $G''(\omega, \varphi)$ ] in the low- $\omega$  side where NR undergoes the terminal flow ( $G' \sim \omega^2$ ,  $G'' \sim \omega^1$ ) [2, 4]. A  
13 totally solid-like rheology [ $G'(\omega, \varphi) > G''(\omega, \varphi)$  within the  $\omega$  range experimentally achieved] is  
14 observed for the compounds filled with PS [ $\varphi_{PS}=0.20$  for the single-filler compounds PS(NR)],  
15 SNF [ $\varphi_{SNF} \geq 0.14$  for the single-filler compounds SNF(NR)<sub>uc</sub> and SNF(NR)<sub>c</sub>], or both [ $\varphi_{PS}=0.20$  and  
16  $\varphi_{SNF}=0.014$  for the two-filler compounds PS(SNF0.014);  $\varphi_{PS}=0.12$  and  $\varphi_{SNF}=0.07$  for the two-  
17 filler compounds SNF(PS0.12)<sub>d</sub>]. Both the uncompatibilized and compatibilized single-filler  
18 compounds, SNF(NR)<sub>uc</sub> and SNF(NR)<sub>c</sub>, show the solid-like rheology at the same  $\varphi_{SNF}$  range while  
19 the single-filler compounds prepared via the dilution method, SNF(NR)<sub>d</sub>, demonstrate the  
20 liquid-like rheology due to the low SNF loadings. The liquid-to-solid transition induced by  
21 nanosized PS can be ascribed to the networking of nanoparticles interconnected by chain  
22 bridges [9-15]. In the SNF compounds, it could also be induced by the formation of a physical  
23 fiber network [16, 17].

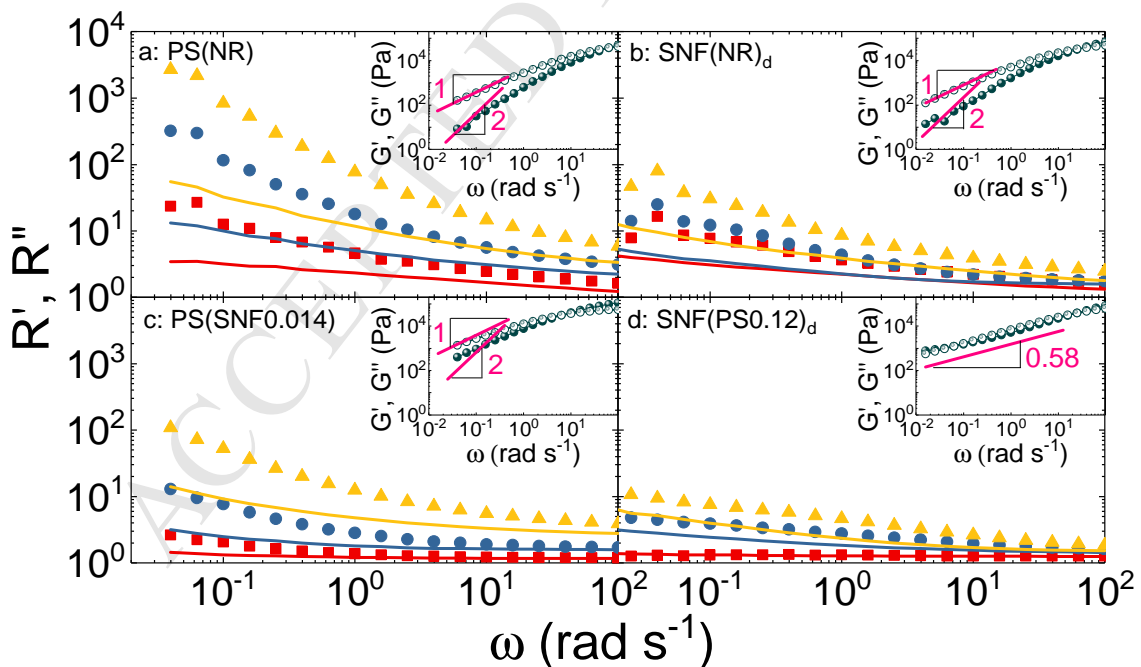


1  
2 **Fig. 1.** Dynamic moduli  $G'(\omega, \varphi)$  (symbols) and  $G''(\omega, \varphi)$  (curves) as a function frequency  $\omega$  for PS(NR),  
3 PS(SNF0.014), SNF(NR)<sub>uc</sub>, SNF(NR)<sub>c</sub>, SNF(NR)<sub>d</sub>, and SNF(PS0.12)<sub>d</sub> from the left to right. The fillers volume  
4 fractions are indicated. The data are horizontally shifted by a factor of  $10^m$  for a clear comparison of the  
5 linear rheology of the different compounds.

6  
7 For the single-filler compounds, both PS and SNF reinforce the NR matrix, as shown in Fig. 2a  
8 and b where relative dynamic moduli,  $R'(\omega, \varphi) = G'(\omega, \varphi) / G'_m(\omega)$  and  $R''(\omega, \varphi) = G''(\omega, \varphi) / G''_m(\omega)$ ,  
9 are plotted as a function of  $\omega$ . Here  $G'_m(\omega)$  and  $G''_m(\omega)$  are storage and loss moduli,  
10 respectively, of the matrix. At given  $\varphi$ , both  $R'(\omega, \varphi)$  and  $R''(\omega, \varphi)$  decrease with increasing  $\omega$   
11 and  $R''(\omega, \varphi)$  is always lower than  $R'(\omega, \varphi)$ . For the two-filler compounds, the first type of filler  
12 (varying loadings) could also reinforce the filled NR matrix (NR filled with the second filler at a  
13 constant loading), as shown in Fig. 2c and d. Furthermore, both  $R'(\omega, \varphi)$  and  $R''(\omega, \varphi)$  become  
14 nearly  $\omega$ -independent in the high- $\omega$  hydrodynamic limit, which is more marked for the two-



1 filler compounds at low  $\varphi$ . The results presented in Fig. 2 reveal a filling-induced hydrodynamic  
 2 to non-hydrodynamic transition with increasing  $\varphi$  and decreasing  $\omega$ . This transition is  
 3 undoubtedly strongly influenced by the filler type and composition. It is clear that both  $R'(\omega, \varphi)$   
 4 and  $R''(\omega, \varphi)$ , characterizing the increments of dynamic moduli of the two-filler compounds  
 5 over the filled NR matrix, are lower than those in the single-filler compounds. For example, the  
 6 reinforcement effect of PS in the two-filler compounds PS(SNF0.014) (Fig 2c) is reduced  
 7 markedly in comparison with that in the single-filler compounds PS(NR) (Fig 2a), by more than  
 8 one order of magnitude at  $\varphi_{PS}=0.20$  at the lowest  $\omega$ , which could be related to the dynamics  
 9 retardation in the filled NR matrix (inset in Fig 2c). In the two-filler compounds SNF(PS0.12)<sub>d</sub>  
 10 whose filled matrix ( $\varphi_{PS}=0.12$ ) behaves critical gel-like [ $G'_m(\omega) \approx G''_m(\omega) \sim \omega^{0.58}$ , inset in Fig 2d]  
 11 due to the filler networking [1, 2, 4], the reinforcement effect of SNF (Fig 2d) becomes much  
 12 lower than that in the single-filler compounds SNF(NR)<sub>d</sub> (Fig 2b). It means that the linear  
 13 rheology of the compounds is strongly influenced by the dynamics of the (filled) matrix.



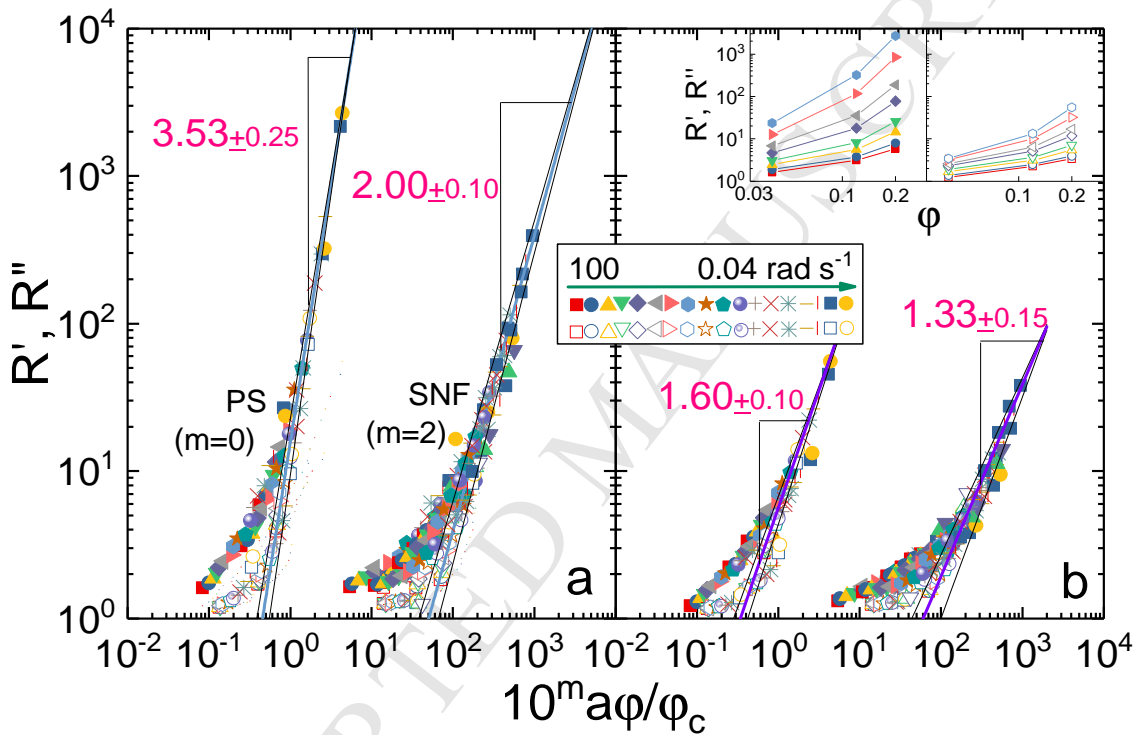
14  
 15

16 **Fig. 2.** Relative dynamic moduli  $R'$  (solid symbols) and  $R''$  (curves) as a function frequency  $\omega$  for PS(NR) (a,  
 17  $\varphi_{PS}=0.04, 0.12, \text{ and } 0.20$ , from bottom to top), SNF(NR)<sub>d</sub> (b,  $\varphi_{SNF}=0.014, 0.035 \text{ and } 0.070$ , from bottom

1 to top), PS(SNF0.014) (c,  $\varphi_{PS}=0.04, 0.12, \text{ and } 0.20$ , from bottom to top) and SNF(PS0.12)<sub>d</sub> (d:  $\varphi_{SNF}=0.014,$   
 2  $0.035 \text{ and } 0.070$ , from bottom to top). The insets show linear rheology of the (filled) matrix, indicating  
 3 the deviation from classic terminal flow law.

4  
 5 While  $R'(\omega, \varphi)$  is usually used to semiempirically discuss the reinforcement mechanism in  
 6 relation to hydrodynamic effect in the “high”- $\omega$  regime at low- $\varphi$ , or the jamming effect in the  
 7 “low”- $\omega$  regime at moderately high- $\varphi$  [2-4, 18-20], no theory could account for  $R''(\omega, \varphi)$ . It is  
 8 revealed recently that the liquid-to-solid transition in polymer nanocomposites in wide ranges  
 9 of  $\varphi$  and  $\omega$  can be accounted for by a time-concentration superposition principle [21-27]. This  
 10 principle allows normalizing both  $R'(\omega, \varphi)$  and  $R''(\omega, \varphi)$  with respect to  $\varphi$  scaled by an  $\omega$ -  
 11 dependent critical filler loading  $\varphi_c(\omega)$ , which is validated in the compounds containing  
 12 nanosized PS, microsized SNF and both. As shown in Fig. 3,  $R'(\omega, \varphi)$  and  $R''(\omega, \varphi)$  [shown in inset  
 13 in Fig. 3 for the single-filler compounds PS(NR) as an example] are normalized onto their  
 14 respective master curves by plotting against  $\varphi/\varphi_c(\omega)$ ; the superposition does not call for any  
 15 vertical shift factors even though the superposed data are somewhat scattered in a narrow range.  
 16 Note that, in the whole  $\varphi/\varphi_c(\omega)$  range achieved, both the reinforcement and dissipation  
 17 effects in the single-filler compounds are more significant than those in the two-filler  
 18 compounds (as shown in Fig. 2). The master curves of the two-filler compounds are shifted  
 19 horizontally so as to overlap those of the single-filler compounds at  $\varphi/\varphi_c(\omega) > 1$  in the non-  
 20 hydrodynamic regime. In this regime, the reinforcement obeys the unique scaling law  
 21  $R'(\omega, \varphi) \sim [\varphi/\varphi_c(\omega)]^x$  predicted by the cluster-cluster aggregation model [1-4, 28-34]. Here  $x$  is a  
 22 critical exponent being usually taken as 4.5 for the reaction-limited cluster-cluster aggregation  
 23 (weak link regime dominated by the floc network) and 3.5 for the diffusion-limited cluster-  
 24 cluster aggregation (strong link regime dominated by individual flocs) in 3D [34]. The  $x$  values  
 25 of the single- and two-filler compounds, PS(NR) and PS(SNF0.014), are the same ( $x \approx 3.50 \pm 0.25$ ),

1 no matter whether SNF ( $\varphi_{\text{SNF}}=0.014$ ) is incorporated or not. Also true are the  $x$  values  
 2 ( $x \approx 2.00 \pm 0.10$ ) of the single-filler compounds  $\text{SNF}(\text{NR})_{\text{uc}}$ ,  $\text{SNF}(\text{NR})_{\text{c}}$ , and  $\text{SNF}(\text{NR})_{\text{d}}$  and the two-  
 3 filler compounds  $\text{SNF}(\text{PS0.12})_{\text{d}}$ , regardless of whether or not PS ( $\varphi_{\text{PS}}=0.12$ ) is incorporated. The  
 4 slopes of the  $R''(\omega, \varphi)$  master curves in the non-hydrodynamic regime are smaller than those of  
 5  $R'(\omega, \varphi)$ , being about  $1.60 \pm 0.10$  for the PS(NR) and PS(SNF0.014) compounds and  $1.33 \pm 0.15$  for  
 6  $\text{SNF}(\text{NR})_{\text{uc}}$ ,  $\text{SNF}(\text{NR})_{\text{c}}$ ,  $\text{SNF}(\text{NR})_{\text{d}}$ , and  $\text{SNF}(\text{PS0.12})_{\text{d}}$  compounds, respectively.

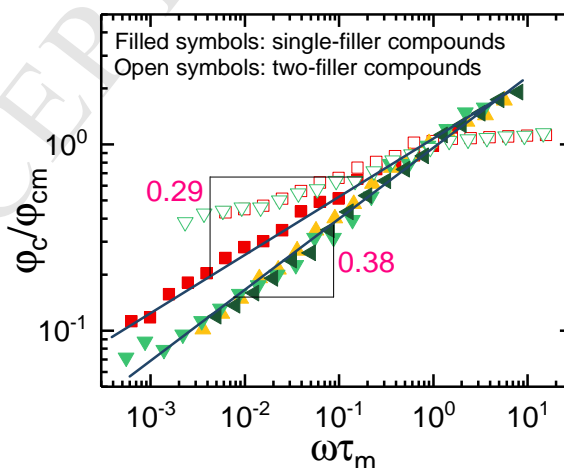


7  
8

9 **Fig. 3.** Relative dynamic moduli,  $R'(\omega, \varphi)$  (a) and  $R''(\omega, \varphi)$  (b), as a function of  $\varphi / \varphi_c$  for the single- (filled  
 10 symbols) and two-filler compounds (open symbols). The master curves are created for the compounds  
 11 with varying  $\varphi$  and  $\omega$ . The data for the single-filler compounds marked as “SNF” includes  $\text{SNF}(\text{NR})_{\text{uc}}$ ,  
 12  $\text{SNF}(\text{NR})_{\text{c}}$ , and  $\text{SNF}(\text{NR})_{\text{d}}$ . The straight lines are drawn according to the scaling law. The data for the  
 13 compounds with varying SNF loadings are shifted rightward by two orders of magnitude for clear display.  
 14 The data for the two-filler compounds are shifted by a factor of  $a$  for overlapping onto that of the single-  
 15 filler compounds. Inset shows  $R'$  (filled symbols) and  $R''$  (open symbols) at eight prescribed frequencies  
 16 (100, 40, 10, 4, 1, 0.4, 0.1, and 0.04  $\text{rad s}^{-1}$ , from bottom to top) as a function of  $\varphi$  for PS(NR).

1

2 In the time-concentration superposition approximation,  $\varphi_c(\omega)$  depicts a unique  $\omega$ -  
 3 dependent hydrodynamic-to-non-hydrodynamic regime transition dominated by the relaxation  
 4 of the matrix.  $\varphi_c(\omega)$  is shown in a normalized form in Fig. 4, in which  $\tau_m$  is the terminal  
 5 relaxation time of pure polymer and  $\varphi_{cm}$  is the  $\varphi_c(\omega)$  value at  $\omega=1/\tau_m$  (Table 1). For the single-  
 6 filler compounds,  $\tau_m$  is determined at reciprocal of frequency at the  $G'_m(\omega)-G''_m(\omega)$  crossover;  
 7 for the two-filler compounds,  $\tau_m$  is determined according to the modified two phase model  
 8 applied to the filled NR matrix [24]. It is interesting that the normalized plot of  $\varphi_c(\omega)/\varphi_{cm}$   
 9 against  $\omega\tau_m$  is sensitive to the filler composition rather than the processing method. For the  
 10 single-filler compounds,  $\varphi_c(\omega)/\varphi_{cm}$  scales like  $(\omega\tau_m)^{0.29}$  for PS and  $(\omega\tau_m)^{0.38}$  for SNF. For two-  
 11 filler compounds in which the polymer dynamics are retarded markedly,  $\varphi_c(\omega)/\varphi_{cm}$  levels off in  
 12 the hydrodynamic regime at  $\omega\tau_m>1$  while it is higher than those of the single-filler compounds  
 13 at  $\omega\tau_m<1$ . The scaling behavior observed at high  $\varphi$  (Fig. 3) works only when the matrix relaxes  
 14 fully in the low- $\omega$  region. In comparison with the single-filler compounds, the coexistence of PS  
 15 and SNF would facilitates the hydrodynamic-to-non-hydrodynamic regime transition due to  
 16 the dynamics retardation effect (Table 1).



17

18 **Fig. 4.** Normalized critical filler loading  $\varphi_c(\omega)/\varphi_{cm}$  as a function of normalized frequency  $\omega\tau_m$  for PS(NR)  
 19 (filled square), PS(SNF0.014) (open square), SNF(NR)<sub>uc</sub> (filled left-triangle), SNF(NR)<sub>c</sub> (filled up-triangle),

1 SNF(NR)<sub>d</sub> (filled down-triangle), and SNF(PS0.12)<sub>d</sub> (open down-triangle).

2

3 In conclusion, both PS and SNF induce the apparent liquid-to-solid transition. Despite of  
4 dimensional differences in the two fillers, this transition could be well accounted for by the  
5 time-concentration superposition principle. The roles of filler are found here to be dual. Filler  
6 invariably retards the dynamics of the mobile rubber phase while the coexistence of two types  
7 of fillers could accelerate the liquid-to-solid transition. However, the presence of one type of  
8 filler does not influence the reinforcement and dissipation effects associated with another  
9 type of filler.

## 10 **Acknowledgements**

11 This work was partially supported by the National Natural Science Foundation of China  
12 (Grant No. 51573157, 51333004, and 51373149), the Natural Science Foundation of Zhejiang  
13 Province, China (Grant No. R14E030003), and the Major Projects of Science and Technology  
14 Plan of Guizhou Province, China (Grant No. (2013) 6016).

## 15 **Appendix A. Supplementary material**

16 Supplementary data associated with this article can be found, in the online version, at  
17 [http://dx.doi.org/10.1016/j.polymer.2017.\\*\\*.\\*\\*\\*](http://dx.doi.org/10.1016/j.polymer.2017.**.***).

## 18 **References**

- 19 [1] Y. Song, M. Du, H. Yang, Q. Zheng, *Acta Polym. Sinica* 22 (2013) 1115-1130.  
20 [2] Y. Song, Q. Zheng, *J. Rheol.* 59 (2015) 155-191.  
21 [3] Y. Song, Q. Zheng, *Crit. Rev. Solid State Mater. Sci.* 41 (2016) 318-346.  
22 [4] Y. Song, Q. Zheng, *Prog. Mater Sci.* 84 (2016) 1-58.  
23 [5] C. G. Robertson, *Rubber Chem. Technol.* 88 (2015) 463-474.  
24 [6] Y.-T. Tsai, J.-Y. Chiou, C.-Y. Liao, P.-Y. Chen, S.-H. Tung, J.-J. Lin, *Compos. Sci. Technol.* 132 (2016) 9-15.  
25 [7] D. Huang, Y. Song, Q. Zheng, *Acta Polym. Sinica* 25 (2015) 542-549.

- 1 [8] C. Nakason, A. Kaesaman, Z. Samoh, S. Homsin, S. Kiatkamjornwong, *Polym. Test.* 21 (2002) 449-  
2 455.
- 3 [9] G. P. Baeza, C. Dessi, S. Costanzo, D. Zhao, S. Gong, A. Alegria, R. H. Colby, M. Rubinstein, D.  
4 Vlassopoulos, S. K. Kumar, *Nat. Commun.* 7 (2016) 11368.
- 5 [10] Q. Chen, S. Gong, J. Moll, D. Zhao, S. K. Kumar, R. H. Colby, *ACS Macro Lett.* 4 (2015) 398-402.
- 6 [11] S. Gan, Z. L. Wu, H. Xu, Y. Song, Q. Zheng, *Macromolecules* 49 (2016) 1454-1463.
- 7 [12] Z. Zheng, Y. Song, H. Xu, Q. Zheng, *Macromolecules* 48 (2015) 9015-9023.
- 8 [13] Z. Zheng, Y. Song, X. Wang, Q. Zheng, *J. Rheol.* 59 (2015) 971-993.
- 9 [14] Z. Zheng, Y. Song, R. Yang, Q. Zheng, *Langmuir* 31 (2015) 13478-13487.
- 10 [15] Y. X. Zhang, M. Zuo, T. Liu, Y. H. Song, Q. Zheng, *Compos. Sci. Techn.* 123 (2016) 39-48.
- 11 [16] A. Kasgoz, D. Akin, A. Durmus, *Compos. Part B: Eng.* 62 (2014) 113-120.
- 12 [17] M. M. Rueda, R. Fulchiron, G. Martin, P. Cassagnau, *Eur. Polym. J.* 93 (2017) 167-181.
- 13 [18] K. Nusser, G. J. Schneider, W. Pyckhout-Hintzen, D. Richter, *Macromolecules* 44 (2011) 7820-7830.
- 14 [19] J. Vermant, S. Ceccia, M. K. Dolgovskij, P. L. Maffettone, C. W. Macosko, *J. Rheol.* 51 (2007) 429-450.
- 15 [20] Y. Song, Q. Zheng, *Polymer Bulletin (In Chinese)* 15 (2013) 22-34.
- 16 [21] Y. Song, L. Zeng, Q. Zheng, *J. Phys. Chem. B* 121 (2017) 5867-5875.
- 17 [22] Y. Song, L. Zeng, A. Guan, Q. Zheng, *Polymer* 121 (2017) 106-110.
- 18 [23] Y. Song, L. Zeng, Q. Zheng, *Chinese J. Polym. Sci.* 35 (2017) 1436-1446.
- 19 [24] Y. Song, Y. Tan, Q. Zheng, *Polymer* 112 (2017) 35-42.
- 20 [25] Y. Song, L. Zeng, Q. Zheng, *Compos. Sci. Techn.* 147 (2017) 39-44.
- 21 [26] Y. Song, A. Guan, L. Zeng, Q. Zheng, *Compos. Sci. Techn.* 151 (2017) 104-108.
- 22 [27] Y. Song, Q. Zheng, *Polymer* 130 (2017) 74-78.
- 23 [28] T. A. Vilgis, G. Heinrich, M. Klüppel. *Reinforcement of Polymer Nano-Composites: Theory,*  
24 *Experiments and Applications.* Cambridge: Cambridge University Press, 2009.
- 25 [29] G. Huber, T. A. Vilgis, *Kautsch. Gummi Kunstst.* 52 (1999) 102-107.
- 26 [30] G. Heinrich, M. Klüppel, T. A. Vilgis, *Curr. Opin. Solid State Mater. Sci.* 6 (2002) 195-203.
- 27 [31] M. Klüppel, *Adv. Polym. Sci.* 164 (2003) 1-86.
- 28 [32] S. Westermann, M. Kreitschmann, W. PyckhoutHintzen, D. Richter, E. Straube, *Physica B* 234 (1997)

- 1 306-307.
- 2 [33] G. Heinrich, M. Kluppel, Adv. Polym. Sci. 160 (2002) 1-44.
- 3 [34] R. Buscall, P. D. A. Mills, J. W. Goodwin, D. W. Lawson, J. Chem. Soc., Faraday Trans. 1: Phys. Chem.
- 4 Condens. Phases 84 (1988) 4249-4260.

ACCEPTED MANUSCRIPT

**Highlights**

- Viscoelasticity of natural rubber compounds varies with nanosilica and microscopic short nylon fiber.
- Linear rheology of the compounds follows time-concentration superpositioning principle.
- The rheological contributions of nanosilica and short nylon fibers are independent of each other.